PHYSICAL REVIEW E VOLUME 50, NUMBER 2 AUGUST 1994

Scale similarity of the velocity structure functions in fully developed magnetohydrodynamic turbulence

Vincenzo Carbone
Dipartimento di Fisica and Consorzio Istituto Nazionale di Fisica della Materia, Universitá della Calabria, 87036 Roges di Rende, Cosenza, Italy

(Received 14 February 1994)

Turbulence theory has been recently enriched by the concept of extended self-similarity introduced by Benzi *et al.* [Phys. Rev. E **48**, R29 (1993)] which showed that an extended scaling range, including both the inertial and the dissipative regions, can be observed when the usual qth-order velocity structure functions are plotted against the structure function of the third order. The same concept has been reviewed by Stolovitzky and Sreenivasan [Phys. Rev. E **48**, R33 (1993)], whose high resolution measurements show the existence of two scaling regions which become increasingly distinct as the order of the velocity structure function increases. In this paper, by using a shell model for three-dimensional magnetohydrodynamic (MHD) turbulence, we show that the extended self-similarity could be an interesting concept also in fully developed MHD turbulence.

PACS number(s): 47.65.+a, 47.27.−i

Interesting features of turbulent flows are represented by the scaling properties of the velocity structure function in the inertial range. This region, in homogeneous and isotropic fully developed turbulence, can be defined as the range of length scales l for which the Kolmogorov relation [1] holds

$$\langle \Delta v^3 \rangle = -\tfrac{4}{5}\langle \epsilon \rangle l. \tag{1}$$

The quantity ϵ represents the energy dissipation rate per unit mass, $\Delta v(l)=v(x+l)-v(x)$ is the usual velocity structure function, and the angle brackets represent spatial averages. The relation (1) can be derived from the Navier-Stokes equation, and is experimentally verified over an interval of scales l which depends on the Reynolds number. Experiments in fluid flows showed the existence of scale invariance measured from a scaling exponent $s(q)$ defined, in the range l where Eq. (1) is satisfied, through $\langle \Delta v^q \rangle \sim l^{s(q)}$ (the symbol $\sim$ means that two quantities have the same scaling law). In the absence of intermittency the linear Kolmogorov scaling law $s(q)=q/3$ holds, whereas $s(q)$ is a nonlinear function of q in the presence of intermittency (see Ref. [2] and references therein). However, for small Reynolds numbers, the calculation of $s(q)$ can be mistaken due to the limited extension of the inertial range. Recently Benzi *et al.* [3] looked for an extension of the range of scale similarity which would be useful in the calculation of the scaling exponents at small Reynolds numbers. Since the relation $\langle |\Delta|^3 \rangle \sim |\langle \Delta v^3 \rangle|$ is verified experimentally, these authors suggest obtaining the scaling exponents through a relation involving the third-order velocity structure function, say $\langle \Delta v^q \rangle \sim \langle |\Delta v|^3 \rangle^{\xi(q)} \sim |\langle \Delta v^3 \rangle|^{\xi(q)}$. Almost surprisingly the log-log plots of $\langle |\Delta v|^q \rangle$ vs $\langle |\Delta v|^3 \rangle$, and those of $|\langle \Delta v^q \rangle|$ vs $|\langle \Delta v^3 \rangle|$, seem to show, for $q \leq 6$, a range of scale similarity which extends well beyond the inertial range as measured from Eq. (1), and includes the dissipation range. From these plots Benzi *et al.* [3] claimed the existence of an extended self-similarity in fully developed turbulence, supposing that the same was true also for magnetohydrodynamic (MHD) turbulence. This analysis has been repeated [4] by using measurements with very long data records. The results show that the large extended self-similarity is not visible for all the values of q. Indeed, for the higher-order velocity structure functions, the inertial range and the dissipative range separate out [4]: a log-log plot of $\langle |\Delta v|^q \rangle$ vs $\langle |\Delta v|^3 \rangle$ (as well as a log-log plot of $|\langle \Delta v^q \rangle|$ vs $|\langle \Delta v^3 \rangle|$), consists of two linear regions, with almost different slopes, joined by a transition region. The difference in the slopes, measured in both ranges, increases as q increases. Even if these measurements [4] seem to bar, for high-order structure functions, the presence of the extended self-similarity, this concept is an interesting and promising tool, and reveals some "hidden" properties of scale similarities in turbulence.

Historically, scale similarities in MHD turbulent flows received less attention with respect to fluid flows. One of the reasons is the fact that the "laboratory measurements" which allow us to obtain information on MHD turbulence are represented by satellite observations of both the velocity **u** and the magnetic **B** fluctuations in the solar wind plasma. In this case, due to the difference in both the nature of the turbulence and the measurements from the ordinary fluid flows, a statistically homogeneous sample of turbulent magnetofluid is limited to data records with a number of sampling points smaller than, for example, that used by Stolovitzky and Sreenivasan [4]. For this reason the higher-order structure functions, as measured in the solar wind plasma, must be handled carefully. Even if this "handicap" is present, the curves analogous to $s(q)$, for the velocity and the magnetic field structure functions, appeared in some papers [5,6]. These analyses represent convincing experimental evidence for the presence of intermittency in MHD turbulence. On the other hand, three-dimensional (3D) MHD simulations [7] showed a multifractal structure, and the results of the p model [8], have been extended to MHD turbulence [9]. Due to the limitation of the measurements in MHD turbulence, we think that the notion of extended self-similarity could be very useful for a better description of the scale similarity and the intermittency in the MHD turbulence.

To check the notion of extended self-similarity, we studied a shell model which describes MHD turbulence [10,11].

Shell models can be heuristically obtained by imposing the general conservation principles of fluid flows, and they mimic the gross features of MHD turbulence [12]. Let us assume that the wave vector space is divided into discrete shells Δ_n (where $n=0,1,\ldots,N$) defined by $k_0 2^{n-1/2} \leq |\mathbf{k}| \leq k_0 2^{n+1/2}$. Each shell has associated a discrete wave vector $k_n=2^n$ (we take $k_0=1$) and two dimensionless real dynamical variables: a discrete velocity field $u_n(t)$ and a magnetic field $b_n(t)=B_n/(4\pi\rho)^{1/2}$ (ρ being the constant plasma mass density). From these fields we can define $Z_n^{\pm}(t)=u_n(t)\pm b_n(t)$, which represent the discrete Elsässer variables, say Alfvénic fluctuations propagating in the opposite direction along the magnetic field of the largest scale. We then assume that $Z_n^{\pm}(t)$ evolve according to a system of equations whose characteristics are similar to the MHD equations when written in the Fourier space [10,12]

$$\frac{dZ_n^{\pm}(t)}{dt}=k_n \sum_{i,j} A_{i,j} Z_{n+i}^{\pm}(t) Z_{n+j}^{\mp}(t) - \nu k_n^2 Z_n^{\pm}(t) + \delta_{n,0} .$$

The parameters $A_{i,j}$ are free constants, ν is a dimensionless dissipative coefficient, and $\delta_{n,0}$ is an external driving force acting on the largest-scale velocity field. Imposing that in the absence of dissipation and forcing terms the system (as well as the original MHD equations) conserves both pseudoenergies $E^{\pm}(t)=\Sigma_n[Z_n^{\pm}(t)]^2$, and assuming that the nonlinear interactions happen only between contiguous shells $(i,j=-1,0,1)$, we obtain

$$\frac{dZ_n^{\pm}}{dt}=k_n A(Z_{n-1}^{\pm} Z_{n-1}^{\mp} - 2Z_{n+1}^{\pm} Z_n^{\mp}) + k_n(Z_{n-1}^{\pm} Z_n^{\mp} - 2Z_{n+1}^{\pm} Z_{n+1}^{\mp}) - \nu k_n^2 Z_n^{\pm} + \delta_{n,0} . \quad (2)$$

The parameter A is the only free constant. The system (2) shares some peculiarities with MHD turbulence, say a power law spectrum, chaotic behavior when ν is varied, and a kind of dynamo effect [10,11]. The statistical properties of MHD equations are almost well described by Eq. (2), while the main difference is represented by the absence of spatial fluctuations within each shell [12]. By looking at Eq. (2), it is a simple matter to show the existence of an unstable fixed point of the Kolmogorov type $Z_n^{\pm} \sim k_n^{-1/3}$. The Alfvén effect has not been explicitly incorporated in the MHD shell model [10,12], thus a $k^{-5/3}$ Kolmogorov-type spectrum for the pseudoenergies is obtained instead of a $k^{-3/2}$ Kraichnan spectrum. Starting from random values of $Z_n^{\pm}$ at $t=0$, we have numerically solved Eq. (2) by using $N=19$ modes, $\nu=10^{-7}$ (the dissipative wave vector is $k_D \sim \nu^{-3/4} \simeq 2^{16}$), and different values of the coupling coefficient A (see Refs. [10,11] for details on the properties of the system when the parameters are varied). In this paper we will present the results obtained for both $A=10^{-2}$ and 0.7. These values of A refer to two different dynamical regimes of Eq. (2). Using the first value of A the system lies on a chaotic attractor, while when $A>0.5$ the attractor changes its nature becoming a nonmagnetic stable fixed point [11]. The integration of the system has been carried out for several time steps thus obtaining, for each variable $Z_n^{\pm}(t)$, a series of 10^7 points on the attractor. This is enough to assure the convergence, at least

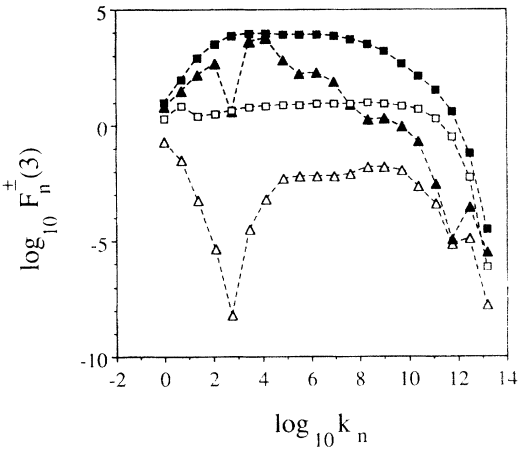

FIG. 1. log-log plots of the spectrum of the quantity $F_n^{\pm}(3)$ which represents $k_n S_n^{\pm}(3)$ (squares) and $k_n G_n^{\pm}(3)$ (triangles). Black symbols refer to the modes S_n^+ and G_n^+, white symbols refer to S_n^- and G_n^-. These plots correspond to $A=10^{-2}$.

for $q \leq 20$, of both the quantities $S_n^{\pm}(q)=\langle |Z_n^{\pm}|^q \rangle$ and $G_n^{\pm}(q)=|\langle (Z_n^{\pm})^q \rangle|$ (angle brackets being time average) which represent the analogs of the velocity structure functions in the shell model framework [13]. Looking at the time evolution of $Z_n^{\pm}$, one can observe the presence of both localized bursts of activity in between periods of slow activity [10] which reflect a highly time intermittent behavior. The intermittency, similar to the behavior of the chaotic nonmagnetic Ohkitami-Yamada shell model [13], seems to be an effect of the chaotic behavior of the model.

Since the system (2) exhibits an unstable fixed point of the Kolmogorov type, we argue that a relation like (1), say $S_n^{\pm}(3) \sim G_n^{\pm}(3) \sim k_n^{-1}$, should exist. In Fig. 1 we show the log-log plots of the quantities $k_n S_n^{\pm}(3)$ and $k_n G_n^{\pm}(3)$ vs k_n obtained in the chaotic, magnetic regime ($A=10^{-2}$). As can be seen, an inertial range is present, and in this range we can calculate the scaling exponents $\xi^{\pm}(q)$ through the relation $S_n^{\pm}(q) \sim k_n^{-\xi^{\pm}(q)}$. The range where $\xi^+(3) \simeq 1.00 \pm 0.01$ extends approximately to the region $2^4 \leq k_n \leq 2^{10}$, while the range in which $\xi^-(3) \simeq 1.00 \pm 0.01$ is shifted to the region $2^7 \leq k_n \leq 2^{13}$. Looking at the spectra of $G_n^{\pm}(3)$ it can be seen that only for $G_n^-(3)$ an inertial range exists. This range is extended to a smaller region $2^8 \leq k_n \leq 2^{11}$ where $\xi^-(3) \simeq 1.00 \pm 0.05$. The strong difference among the spectra of $S_n^{\pm}(q)$ and $G_n^{\pm}(q)$, which appears in a very limited form in the measurements on real fluid flows, is due to the cancellations occurring on the average, for even q, in the calculation of $G_n^{\pm}(q)$. The difference among the modes S_n^+ and S_n^-, as well as among G_n^+ and G_n^-, is due to the initial value of the cross helicity (defined as $Z_n^+ - Z_n^-$). In fact, different initial values for the fields give rise to different spectra for the structure functions. It is worthwhile to remark that the higher-order structure functions $S_n^{\pm}(q)$ (say, for $q \geq 6$) show oscillations at some length scales, whose amplitude is however small as compared to the "violent" oscillations seen in $G_n^{\pm}(q)$. The presence of oscillations in $S_n^{\pm}(q)$ is a "genuine" effect of the chaotic shell models, being evident also in the Ohkitami-Yamada model, and seems to be caused by a

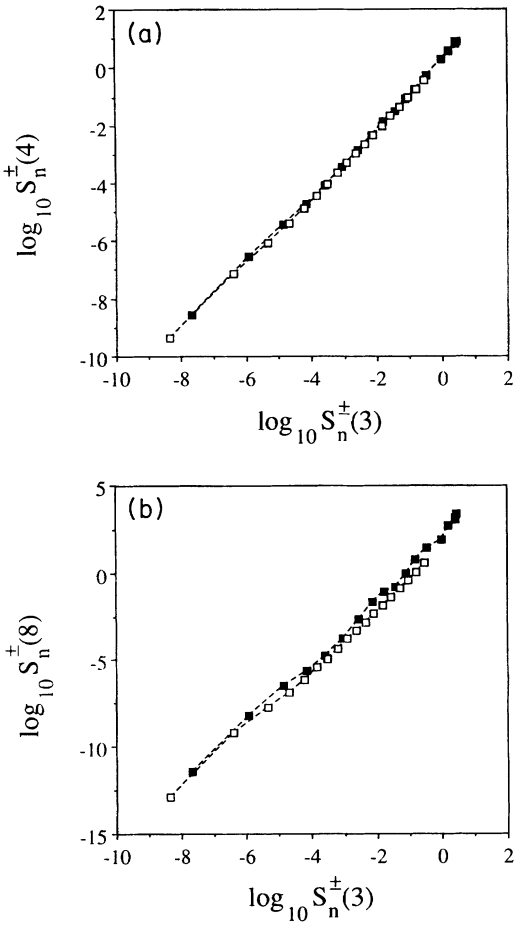

FIG. 2. log-log plots of $S_n^{\pm}(q)$ vs $S_n^{\pm}(3)$ for $q=4$ (a) and $q=8$ (b). Black squares correspond to S_n^{+}, white squares correspond to S_n^{-}. These plots correspond to the chaotic magnetic attractor obtained for $A=10^{-2}$.

lacunarity of fractal sets [14]. By changing the nature of the attractor (say for $A>0.5$) an inertial range is well visible for $S_n^{\pm}$, while the oscillations disappear for all the values of q. On the contrary, $G_n^{\pm}$ show the same oscillating behavior we have evidenced.

We have looked at the scaling exponents $\chi^{\pm}(q)$ through a relation similar to that suggested in [3], say

$$S_n^{\pm}(q) \sim [S_n^{\pm}(3)]^{\chi^{\pm}(q)}.$$

log-log plots of $S_n^{\pm}(q)$ vs $S_n^{\pm}(3)$ in the case $A=10^{-2}$ (chaotic, magnetic attractor) including both the inertial and the dissipative ranges are shown in Fig. 2 for two different values of q. An extended similarity range is clearly visible in the plot for $q=4$ [Fig. 2(a)]; this happens for both S_n^{+} and S_n^{-} and the same behavior is visible at least for $q \leq 6$. This range of scale similarity extending beyond the inertial range and including the dissipative range is what is originally found in Ref. [3]. For the higher values of q [Fig. 2(b) another behavior becomes evident, that is, the curves $S_n^{\pm}(q)$ vs $S_n^{\pm}(3)$ present some oscillations around a linear scaling law. A similar behavior is visible for all $q>6$. The amplitude of

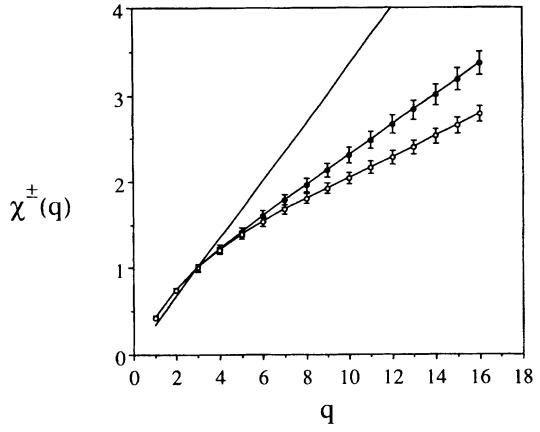

FIG. 3. Scaling exponents $\chi^{+}(q)$ (black symbols) and $\chi^{-}(q)$ (white symbols) vs q, along with the Kolmogorov scaling law $q/3$ (full line). The error bars are also shown.

these oscillations increases slowly when q increases, thus resulting in a slowly increasing error in the determination of the scaling exponents $\chi^{\pm}(q)$. From Fig. 2 we can see that the oscillations are more evident for $S_n^{\pm}(q)$. Actually the log-log plots of $S_n^{\pm}(q)$ vs k_n show oscillations with amplitudes which extend up to two decades, while the oscillations seen in Fig. 2(b) have a very small extension. In Fig. 3 we report the scaling exponents $\chi^{\pm}(q)$ as a function of q. As can be seen, the scaling exponents are the same as far as the range $q \leq 5$ is considered, but as q increases there is an evident difference between χ^{+} and χ^{-}. The extended self-similarity is visible for all the values of the coupling coefficients $A<0.5$, while for the $A>0.5$ some differences can be found. In Fig. 4 we show the log-log plots of $S_n^{\pm}(q)$ vs $S_n^{\pm}(3)$ in the case $A=0.7$ (stable fixed-point, nonmagnetic attractor). The presence of the extended similarity range is distinctly visible because a well defined linear scale is extended both in the inertial and in the dissipative ranges. The linear range is very well defined and the calculation of the scaling exponents can be carried out without errors. This is

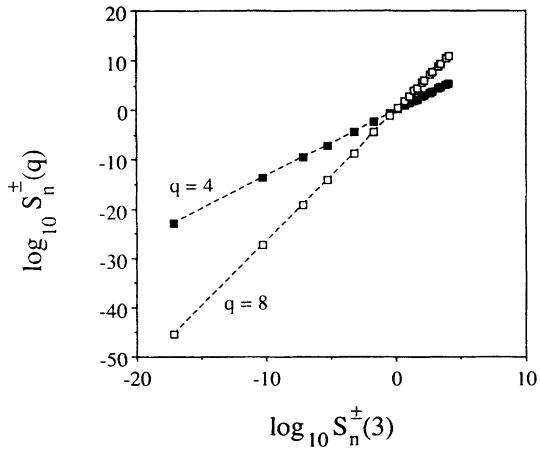

FIG. 4. log-log plots of $S_n^{\pm}(q)$ vs $S_n^{\pm}(3)$ for $q=4$ (black squares) and $q=8$ (white squares). These plots correspond to the nonchaotic nonmagnetic attractor obtained for $A=0.7$.

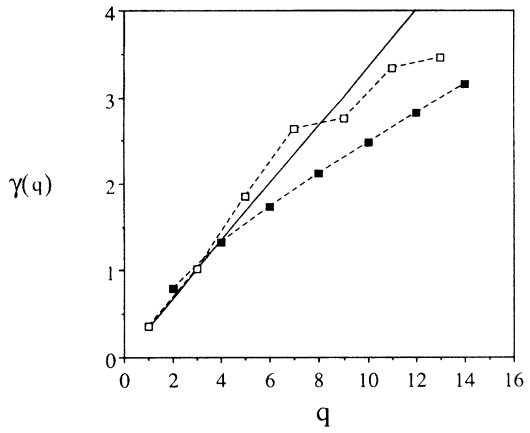

FIG. 5. Scaling exponents $\gamma(q)$ vs q, along with the Kolmogorov scaling law $q/3$ (full line). The odd-order (white squares) and even-order (black squares) exponents fall on different curves.

due to the absence of oscillations in the structure functions. However, in this case we found that the scaling exponents follow a linear Kolmogorov scaling law, say $\chi^+(q)=\chi^-(q)=q/3$, that is, the time intermittency disappears in the nonchaotic case. Similar results can be found for different values of $A>0.5$. Since the values of $G_n^{\pm}(q)$ do not show a clear scale similarity, the log-log plots of $G_n^{\pm}(q)$ against $G_n^{\pm}(3)$ in the extended region do not exhibit any particular behavior. Rather we have calculated the scaling exponents $\gamma(q)$, through the relation $G_n^-(q)\sim k_n^{\gamma(q)}$, only in the small inertial range $2^6\leq k_n\leq 2^{11}$. In Fig. 5 we show the plots of $\gamma(q)$ vs q. The striking feature of this figure is represented by the fact that the odd-order exponents fall on a curve that is distinct and higher than the curve which relates the even-order exponents. This typical behavior, which in the shell model could be seen as a naive result due to the limitation of the scaling range, has also been found [4] as a true result in fluid flow measurements.

A last remark concerns the sensitivity of our results to the precise value of the initial cross helicity. We found that the presence of the extended scale similarity, which is visible for all the values of A, is also visible for all the initial values of the cross helicity. By changing the initial cross helicity the only difference we found was in the values of the scaling exponents $\chi^{\pm}(q)$. Indeed when $A<0.5$ different values of $Z_n^+(0)-Z_n^-(0)$ give rise to different scaling exponents. When $A>0.5$ the (nonmagnetic) attractor has zero cross helicity and we found $\chi^+(q)=\chi^-(q)=q/3$ for all the initial values. Since to our knowledge there is no analysis of the extended self-similarity using nonmagnetic shell models, a particularly interesting case in the MHD model is obtained by imposing zero initial cross helicity. Indeed, since the external force in Eq. (2) acts only on the velocity field, when $Z_n^+(0)=Z_n^-(0)$ the system (2) reduces to a nonmagnetic shell model [12]. In this case, for all the values of A, we found absence of intermittency, absence of oscillations of $S_n^{\pm}(q)$, while the extended self-similarity is well visible for all the values of q. In conclusion, we showed that a kind of extended self-similarity is detectable in the results of a shell model for MHD turbulence. Since the model is obtained by imposing only conservation principles, we think that the concept of extended self-similarity is a basic property of fluid flows. We argue that our results could be extended to MHD turbulence in the solar wind plasma. Experiments from this perspective are currently in progress.

[1] A. N. Kolmogorov, Dokl. Akad. Nauk. SSSR **30**, 301 (1941).
[2] C. Meneveau and K. R. Sreenivasan, J. Fluid Mech. **224**, 429 (1991).
[3] R. Benzi, S. Ciliberto, R. Tripiccione, C. Baudet, F. Massaioli, and S. Succi, Phys. Rev. E **48**, R29 (1993).
[4] G. Stolovitzky and K. R. Sreenivasan, Phys. Rev. E **48**, R33 (1993).
[5] L. F. Burlaga, J. Geophys. Res. **96**, 5847 (1991).
[6] E. Marsch and S. Liu, Ann. Geophys. (Gauthier-Villars) **11**, 227 (1993).
[7] A. Brandenburg, I. Procaccia, D. Segel, and A. Vincent, Phys. Rev. A **46**, 4819 (1992).
[8] C. Meneveau and K. R. Sreenivasan, Phys. Rev. Lett. **59**, 1424 (1987).
[9] V. Carbone, Phys. Rev. Lett. **71**, 1546 (1993).
[10] C. Gloaguen, J. Léorat, A. Pouquet, and R. Grappin, Physica D **17**, 154 (1985).
[11] R. Grappin, J. Léorat, and A. Pouquet, J. Phys. (Paris) **47**, 1127 (1986).
[12] V. Carbone and P. Veltri, Phys. Fluids A **1**, 420 (1989).
[13] M. H. Jensen, G. Paladin, and A. Vulpiani, Phys. Rev. A **43**, 798 (1991).
[14] D. Pisarenko, L. Biferale, D. Courvoisier, U. Frisch, and M. Vergassola, Phys. Fluids A **5**, 2533 (1993).